

# Redox Property of Vanadium Oxide and Its Behavior in Catalytic Oxidation

Young Ho Kim<sup>†</sup> and Ho-In Lee<sup>\*</sup>

*School of Chemical Engineering, Seoul National University, Seoul 151-742, Korea*

*<sup>†</sup>Department of Chemical Engineering, Kunsan National University, Chonbuk 573-701, Korea*

*Received June 25, 1999*

Structure and their redox property of the vanadium oxides prepared by decomposing  $\text{NH}_4\text{VO}_3$  at various temperatures were studied by XRD, SEM, XPS, and temperature programmed reduction/temperature programmed oxidation (TPR/TPO) experiment. All TPR profiles have two sharp peaks in the temperature range 650–750 °C, and the area ratio of the two sharp peaks changed from sample to sample. There were three redox steps in TPR/TPO profiles. The oxidation proceeded in the reverse order of the reduction process, and both the reactions proceeded *via* quite a stable intermediates. The changes of the morphological factor ( $I_{(101)}/I_{(010)}$ ), the ratio of  $\text{O}_{1s}$  peak area ( $\text{O}_{1s}(\alpha)/\text{O}_{1s}(\beta)$ ) in the XPS results, and the ratio of hydrogen consumption in TPR profiles with various vanadium oxides showed the distinct relationship between the structural property and their redox property of vanadium oxides. The change of the specific yield of phthalic anhydride with various vanadium oxides showed a very similar trend to those of the peak area ratio in TPR profiles, which meant that the first reduction step related to the partial oxidation of *o*-xylene on the vanadium oxide catalyst.

## Introduction

Vanadium oxide is a well-known catalyst among various metal oxides, and so many fundamental studies have been developed wide-spreadingly centering around catalytic oxidation. As a commercial catalyst for selective oxidation of benzene, naphthalene, *o*-xylene or methanol, vanadium oxide has been watched for a long time. Recently it is also used in the preparation of maleic anhydride from 1-butene or *n*-butane. So much endeavor for finding the reason why the vanadium oxide showed good catalytic activity for selective oxidation has been made, and the surface morphology of vanadium oxide particles, the shear structure of vanadium oxide, or the V=O active species have been main issues for discussion.

According to many studies, the partial oxidation on vanadium oxides was considered to be based on the redox mechanism (Mars-van Krevelen cycle),<sup>1–4</sup> and the active sites were reported to be the  $\text{V}^{5+}=\text{O}$  species.<sup>5–8</sup> The  $\text{V}^{5+}=\text{O}$  bonds are known to be on the (010) plane of vanadium oxides.<sup>9</sup> The oxygen species of  $\text{V}^{5+}=\text{O}$  are readily exchanged with gas phase oxygen, but it is less easy to exchange oxygens between  $\text{V}^{5+}=\text{O}$  and V-O-V in bulk vanadium oxides.<sup>10</sup>

Gasior and Machej<sup>11</sup> investigated the influence of the grain morphology of vanadium oxide on its activity and selectivity for the partial oxidation of *o*-xylene to phthalic anhydride. They found that the selectivity to phthalic anhydride was correlated with the relative contribution of the (010) planes. And they concluded that the active sites responsible for the selective oxidation of *o*-xylene to phthalic anhydride are on the (010) planes of  $\text{V}_2\text{O}_5$  and those for full oxidation on the planes perpendicular to it.

In the present work, we investigated the redox property of vanadium oxides which were prepared with different contribution of (010) planes, using temperature programmed reduction/temperature programmed oxidation technique. We

will focus on the relationship between the redox property and structural property or catalytic activity of vanadium oxides. Partial oxidation of *o*-xylene was chosen as a model reaction for the test of catalytic activity.

## Experimental Section

**Catalyst preparation and characterization.** Six vanadium oxide samples of different grain morphologies were used in this experimental study. Samples were obtained from ammonium metavanadate (Junsei, GR) which was heated for 6 hours at different temperatures (Table 1). V-1, V-2, and V-3 were calcined below melting point (675 °C), and V-4, V-5, and V-6 were calcined above it. All samples were subsequently cooled in the oven, but V-4 was quickly cooled down in ambient air at room temperature. The samples were characterized using BET surface area analyzer (Quantachrome, Quantasorb QS-11), X-ray diffractometry (Rigaku, D/MAX-A), scanning electron microscopy (Jeol, JSM-35), X-ray photoelectron spectroscopy (Perkin-Elmer, PHI 558) was used to differentiate surface oxygen species on vanadium

**Table 1.** Calcination Temperatures, BET Surface Areas and Morphological Factors of Various Vanadium Oxides (All samples were calcined for 6 hours in ambient air.)

Catalysts	Calcination temperature (°C)	BET surface area (m <sup>2</sup> /g)	Morphological factor ( $I_{(101)}/I_{(010)}$ ) <sup>b</sup>
V-1	350	4.0	0.64
V-2	500	2.5	0.41
V-3	660(just before m.p.)	1.1	0.08
V-4	690(just after m.p.) <sup>a</sup>	0.5	0.01
V-5	800	1.1	0.09
V-6	1000	1.0	0.13

<sup>a</sup>After just melted at 690 °C, it was quickly cooled down in air at room temperature. <sup>b</sup>Intensity ratio of XRD peaks for (101) plane and (010) plane

oxides.

**Temperature programmed reduction/oxidation (TPR/TPO).** TPR and TPO measurements of the samples were performed using a similar apparatus described in ref. 12. Quartz tube ( $\phi$  6 mm) with a fused-quartz filter at the center was used as a reactor. Reducing gas mixture for TPR experiment was 5%  $H_2/N_2$ , and the trace of oxygen in the reducing gas was removed by oxy-trap. For TPO experiment 5%  $O_2/He$  was used as oxidizing gas mixture. Total gas flow rate was constant at 30  $cm^3$  (NPT)/min and the sample size was always 30 mg. Reactor was heated at a linear programmed rate (10 K/min) from room temperature to 1073 K.

**o-Xylene partial oxidation.** The catalytic activity in o-xylene oxidation was measured in an isothermal continuous flow fixed-bed reactor using air as an oxygen source. The apparatus and analysis conditions were described in detail elsewhere.<sup>13</sup> The reactant gas mixture was obtained by saturation of the air stream with o-xylene. The catalytic tests were carried out under the following conditions: air/o-xylene mole ratio, 100; liquid-hourly space velocity (LHSV), 50 L-feed/hr g-cat; amount of catalyst, 100 mg; reaction temperature, 450 °C. Reaction products were analyzed using FID (Packard, Model 438) for partial oxidation products and TCD (Yanaco, Model G1800T) for full oxidation products at the same time.

## Results and Discussion

**Structural change with various calcination temperatures.** Vanadium oxide samples made by different calcination temperatures showed structural differences each other apparently. Scanning electron micrographs of the six samples are shown in Figure 1. Samples calcined below melting point (V-1 to V-3) were agglomerates of small grains of poorly defined shape, which grew to a needle-like crystal with the rise of calcination temperature. But other samples above melting point showed a multilayer structure of sheets. Specially, V-4 consisted of well-developed plate-like grains with large faces. V-5 and V-6 seemed to be small fractures of V-4.

X-ray diffraction (XRD) patterns were recorded by using Ni-filtered  $Cu K\alpha$  radiation in order to find some crystallographic differences between samples. The XRD patterns of various vanadium oxides are shown in Figure 2. Vanadium oxides calcined below 500 °C showed the characteristic  $V_2O_5$  peaks at  $2\theta - 20.3^\circ$  ((010) plane),  $26.2^\circ$  ((101) plane), and  $31.0^\circ$  ((400) plane), respectively. Also other samples calcined near the melting point showed the characteristic  $V_2O_5$  peaks, but the ratio of peak intensities changed remarkably. V-3 or V-4 showed a large  $2\theta - 20.3^\circ$  peak, and it meant that vanadium oxides calcined near the melting point had much (010) plane than other samples.

The crystallographic structure of stoichiometric  $V_2O_5$  is built up from distorted trigonal bipyramids,  $VO_5$  unit cell, sharing edges to form zigzag chains along [001] and cross-linked along [100] through shared corners.<sup>14</sup> So the structure forms 2-dimensional sheets, which are weakly linked each

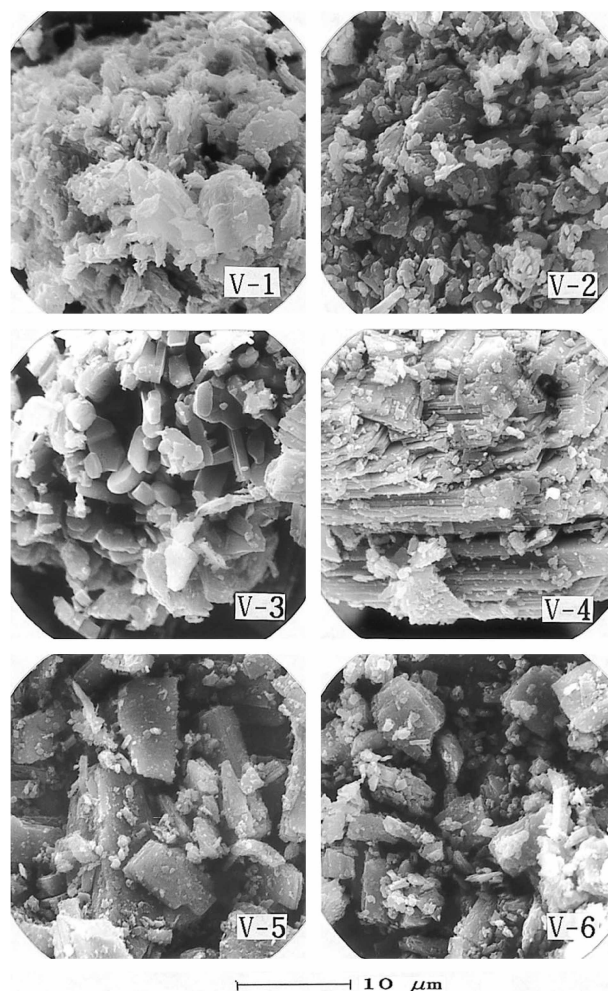


Figure 1. Scanning electron micrographs of various vanadium oxides showing the surface morphologies;  $\times 3,000$ .

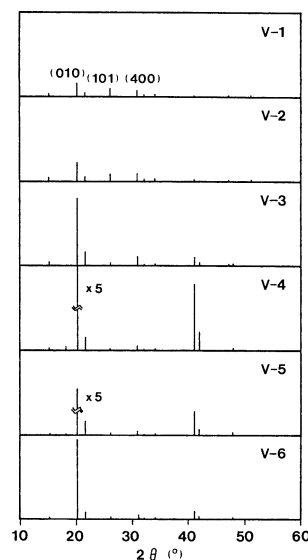


Figure 2. X-ray diffraction patterns of various vanadium oxides.

other *via* oxygen atoms. When vanadium oxides are crystallized from their melt solution, it is likely that the most stable structure, namely, sheets along (010) plane can be well-

developed selectively.

Structural change of vanadium oxide samples can be discussed by the analysis of peak intensity ratio of x-ray diffraction patterns. Ziolkowski and Janas<sup>15</sup> calculated the intensity ratio,  $I_{(101)}/I_{(010)}$  (they called it morphological factor), and they used it as a measure of the ratio of the two planes formed in a bulk vanadium oxide. Morphological factors of various vanadium oxides are shown in Table 1. In the case of orthorhombic single crystal  $V_2O_5$ , the ideal value of  $I_{(101)}/I_{(010)}$  is 0.90.<sup>16</sup> V-1 and V-2 had similar values to single crystal, but the vanadium oxides which were calcined near the melting point or above it had very low  $I_{(101)}/I_{(010)}$  values. Specially, V-4 had a structure which was formed with almost (010) plane only, and we thought that the sheets of V-4 in the scanning electron micrographs corresponded to this plane.

**Redox property of vanadium oxides.** Temperature programmed reduction (TPR) profiles of various vanadium oxides which were calcined at different temperatures are shown in Figure 3. All profiles had two sharp peaks in the temperature range of 650–750 °C, and reduction proceeded successively after 750 °C. The peak temperatures in TPR profiles shifted gradually to low value as the calcination temperature increased. Of the two sharp reduction peaks, labelling low temperature one  $\alpha$  and high temperature one  $\beta$ , we could find that the peak intensity ratio ( $I_{\alpha}/I_{\beta}$ ) increased from V-1 through V-4 and then decreased from V-4 through V-6. Thus, V-4 showed maximum  $I_{\alpha}/I_{\beta}$  value.

Multiple reduction peaks in TPR profiles mean that reduction proceeds *via* several steps. It is clear that vanadium oxides have more than two reduction steps from the results of Figure 3. On the reduction of vanadium oxide, oxygen vacancies are formed at the surface. When the concentration of these vacancies surpasses a certain critical value, they aggregate into a vacancy disc, called shear plane. Part of vanadium oxide may shear so that along the shear plane the

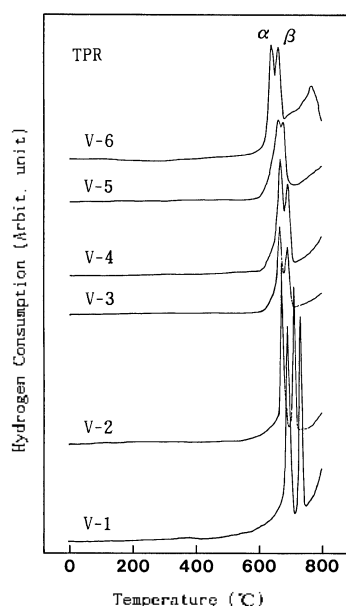


**Figure 3.** TPR profiles measured for various vanadium oxides (heating rate=10 K/min, reducing gas mixture=5%  $H_2/N_2$ ).

linkage between trigonal bipyramids is changed from corner-sharing into edge-sharing.<sup>17</sup> So another stable structure is formed, which is stoichiometrically different from original structure. It is not clear that when this transformation happens or how much concentration of oxygen vacancies it needs to initiate this change. However, we thought that the intermediates of vanadium oxide undergone reduction steps in TPR profiles had relatively stable structure.

In order to get further insight about this point we made a vanadium oxide sample (V-2) be reduced step by step, and the results are shown in Figure 4. Vanadium oxide reduced only to  $\alpha$  step (profile (a) in Figure 4) gave a TPR profile like (b). It showed only one peak at 728 °C, but it was broader than expected. The peak temperature in profile (b) corresponded to  $\beta$  peak in Figure 3 (V-2) exactly. When the vanadium oxide was reduced to  $\beta$  step, it gave a TPR profile like (c). Reduction proceeded only after 750 °C. These results mean that the structure of vanadium oxide formed on the first reduction step  $\alpha$  is quite a stable one, and it is not recovered to the original structure in oxygen-free atmosphere. Another very stable structure was also formed after the second reduction step  $\beta$ .

The sharp reduction peaks seemed to be related to the shear transformation of vanadium oxides. On the first reduction step  $\alpha$  only a sort of oxygens were removed by the reaction with hydrogen. So a sort of shear planes were formed, and the first shear transformation occurred. With the rise of temperature, other sorts of oxygens were removed, and the second shear transformation could take place. And the two kinds of oxygens did not exchange each other. But some of the second oxygen seemed to be diffused to other oxygen vacancies, which made the peak in profile (b) a little wide, but it was not severe. All reduced vanadium oxides could recover their original structure, when they were oxidized for 1 hour at 500 °C in oxygen atmosphere. It is shown in profile (d) of Figure 4.

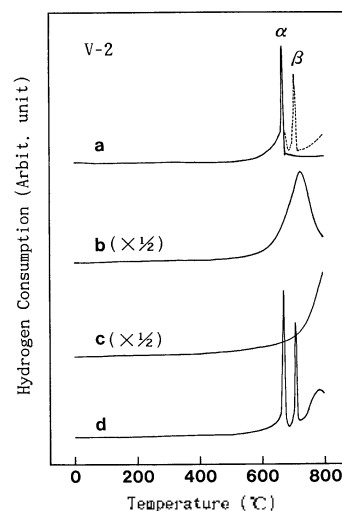


**Figure 4.** TPR profiles measured step by step for sample V-2. (a) partial reduction to the first reduction step, (b) after (a), (c) after the partial reduction to the second reduction step, and (d) after oxidation at 500 °C for 1 hour in  $O_2$  atmosphere.

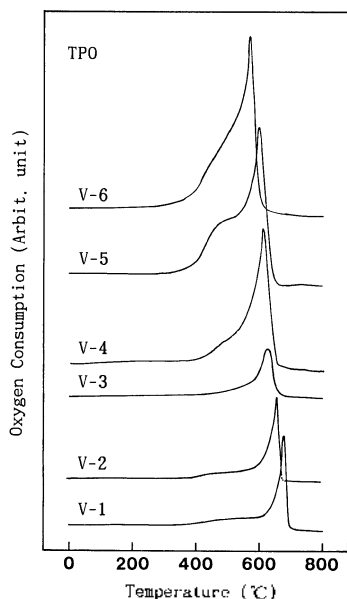


**Figure 5.** TPO profiles measured for various vanadium oxides (heating rate=10 K/min, oxidizing gas mixture=5% O<sub>2</sub>/He).

Temperature programmed oxidation (TPO) profiles of the six samples are shown in Figure 5. They were obtained immediately after the TPR experiments, respectively. In all the TPO profiles, oxidation began at 400 °C and finished at 700 °C, and in the range of the temperature roughly two steps of oxidation appeared. However, we have been afraid of existing of another oxidation step from the peak shape in the TPO profiles. Because the second peak was severely asymmetric, it was possibly expected that there might be another peak between the two peaks.

We thought that TPO would proceed in the reverse order of TPR. It is reasonable that there will be three steps of oxidation in TPO profiles, because there were two sharp reduction peaks and the last reduction step after 750 °C in TPR profiles. We could prove it from the following experimental work. We obtained TPR profiles of the vanadium oxide (V-2) which were oxidized step by step, and the results are shown in Figure 6. In the first place, vanadium oxide (V-2) was fully reduced to 800 °C, and it was partially oxidized to 510 °C by TPO (profile (a) in Figure 6), expecting only the first oxidation step to be finished at this temperature. The TPR profile of this partially oxidized vanadium oxide is shown in Figure 6 (profile (b)). There were not the two sharp peaks, and only the third reduction step began at 750 °C. It means that the first oxidation step in TPO profiles relates to the third reduction step in TPR profiles. The same species of oxygen was related in both reduction and oxidation.

When the reduced vanadium oxide was oxidized to 610 °C by TPO (profile (c)), expecting the first and the second oxidation step to be finished, the two sharp  $\alpha$  and  $\beta$  peaks appeared in TPR (profile (d)). We wanted the reduced vanadium oxide to be oxidized only to the second step exactly, but it was not perfect. So a small  $\alpha$  peak appeared. Anyway, the second oxidation step in TPO related to the second reduction step in TPR, thus, the third oxidation step related

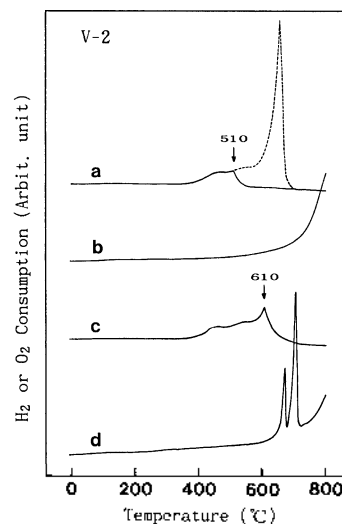
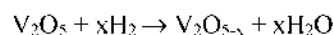


**Figure 6.** TPR profiles measured step by step for sample V-2. (a) partial oxidation to the first oxidation step. (b) after (a). (c) partial oxidation to the second oxidation step. and (d) after (c).

to the first reduction step.

From the above results, it is very clear that there are three oxidation steps in TPO profiles. The oxidation proceeds in the reverse order of reduction process, and both the reactions proceed *via* quite a stable structure. Many of stable structures, such as V<sub>2</sub>O<sub>5</sub>, V<sub>3</sub>O<sub>7</sub>, V<sub>4</sub>O<sub>9</sub>, V<sub>6</sub>O<sub>13</sub>, V<sub>2</sub>O<sub>4</sub>, and V<sub>2</sub>O<sub>3</sub> have been reported.<sup>14</sup> So the partially reduced or oxidized vanadium oxides are expected to have one of these stoichiometries.

**The relationship between the structural change and the redox property of vanadium oxides.** It was very curious why the intensity ratio ( $I_{\alpha}/I_{\beta}$ ) of the two sharp peaks in TPR profiles changed from sample to sample. We expected the ratio would be related to the original structure of the samples, because the change of the ratio showed a similar trend to that of the morphological factor. The peak area in TPR profiles is equal to the amount of hydrogen consumption on the reduction step. Hydrogen molecules are consumed to remove the lattice oxygen of vanadium oxide as the following reaction.



We could calculate the amount of hydrogen consumption with calibrating the peak area previously. The amounts of hydrogen consumption of the two sharp peaks ( $\alpha$  and  $\beta$ ) and the area ratio,  $A(\alpha)/A(\beta)$ , are listed in Table 2. It showed that the amount of hydrogen consumption decreased with the rise of calcination temperature. But the area ratio showed the maximum value at V-4.

On the assumption that the initial structure of vanadium oxide was a stoichiometric V<sub>2</sub>O<sub>5</sub>, we could determine the oxidation states of partially reduced vanadium oxides. The amount of hydrogen to remove all the lattice oxygen in the sample was calculated as  $8.247 \times 10^{-6}$  mole because the sample size used in TPR experiment was always 30 mg. Oxidation states shown in Table 2 were based on this value.

**Table 2.** Hydrogen Consumption of the Two Reduction Peaks in TPR Profiles and the Area Ratio of  $O_{1s}$  Peaks in XPS Results

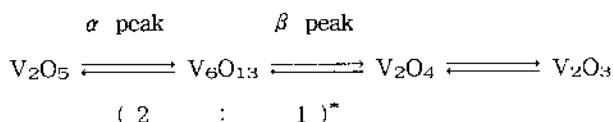
catalysts		V-1	V-2	V-3	V-4	V-5	V-6
$\alpha$ peak	$T_{\alpha}$ ( $^{\circ}\text{C}$ )	695	676	669	676	672	642
	$\text{H}_2$ consumption ( $10^{-5}$ mol)	15.22	12.21	11.16	12.57	8.11	8.22
	Oxidation state <sup>a</sup>	$\text{V}_2\text{O}_{4.08}$	$\text{V}_2\text{O}_{4.26}$	$\text{V}_2\text{O}_{4.32}$	$\text{V}_2\text{O}_{4.21}$	$\text{V}_2\text{O}_{4.51}$	$\text{V}_2\text{O}_{4.50}$
	$\Lambda(\alpha)/\Lambda(\beta)$	1.44	1.66	1.78	1.92	1.22	0.98
$\beta$ peak	$T_{\beta}$ ( $^{\circ}\text{C}$ )	736	714	692	699	691	662
	$\text{H}_2$ consumption ( $10^{-5}$ mol)	10.55	7.37	6.28	6.56	6.65	8.35
	Oxidation state <sup>a</sup>	$\text{V}_2\text{O}_{3.41}$	$\text{V}_2\text{O}_{3.81}$	$\text{V}_2\text{O}_{3.94}$	$\text{V}_2\text{O}_{3.81}$	$\text{V}_2\text{O}_{4.11}$	$\text{V}_2\text{O}_{3.99}$
	$O_{1s}(\alpha)/O_{1s}(\beta)^b$	0.24	0.37	0.57	0.65	0.34	0.26

<sup>a</sup>Calculated under the assumption that initial vanadium oxide were stoichiometric  $\text{V}_2\text{O}_5$ . <sup>b</sup>XPS results

The oxidation states of vanadium oxides which were partially reduced to  $\alpha$  step were given in the range of  $\text{V}_2\text{O}_{4.08}$ - $\text{V}_2\text{O}_{4.51}$ . All samples showed the two sharp reduction peaks in the same temperature range in the TPR profiles, which means that a similar structural change has occurred on the same reduction step in all samples. So the intermediates of vanadium oxides undergone same reduction step were expected to have same structure in all samples. If the initial oxidation states of vanadium oxides were exactly  $\text{V}_2\text{O}_5$ , all samples would show same amount of hydrogen consumption. But Table 2 showed various values of hydrogen consumption, which means that initial structure of vanadium oxide samples are not all alike to stoichiometric  $\text{V}_2\text{O}_5$ .

The average oxidation state of vanadium oxide which was reduced to  $\alpha$  step was  $\text{V}_2\text{O}_{4.32}$ , which corresponded to  $\text{V}_6\text{O}_{13}$ .  $\text{V}_6\text{O}_{13}$  is a very stable structure among various vanadium oxides, and it has been reported frequently by several authors.<sup>17-19</sup> Specially, Dziembaj<sup>20</sup> reported that  $\text{V}_6\text{O}_{13}$  was the only shear structure in the range of  $\text{V}_2\text{O}_5$ - $\text{V}_2\text{O}_4$ . Vanadium oxide which was reduced to  $\beta$  step showed the average oxidation state of  $\text{V}_2\text{O}_{3.86}$  in Table 2. The most stable structure of vanadium oxide around this value is  $\text{V}_2\text{O}_4$ . If the vanadium oxide were reduced further, it should go to  $\text{V}_2\text{O}_3$ , which is the next stable structure. We could arrange the redox steps shown in Figure 3 and Figure 5 as the following Scheme 1.

The ratios of hydrogen consumption,  $\Lambda(\alpha)/\Lambda(\beta)$  were given in the range of 0.98-1.92 in Table 2. If the vanadium oxide had the reduction step of  $\text{V}_2\text{O}_5 \rightarrow \text{V}_6\text{O}_{13} \rightarrow \text{V}_2\text{O}_4$  as



**Scheme 1.** Redox steps of vanadium oxides. \*\* means the theoretical ratio of hydrogen consumption.

Scheme 1, the ratio of hydrogen consumption should have 2.00 theoretically. V-3 and V-4 had very similar values but other samples showed some discrepancy. As told previously, it was caused by the difference of the initial structure among samples. Both the changes of  $A(\alpha)/A(\beta)$  and morphological factor showed a similar trend. In other words, the samples which had more (010) plane showed large  $A(\alpha)/A(\beta)$  values. It means that a sort of oxygen on the (010) plane relates to the reduction step  $\alpha$  or  $\beta$ . There are three sorts of oxygen in bulk  $\text{V}_2\text{O}_5$ , which have different V-O bond lengths, and the oxygens of the shortest bond length (V-O species) were exposed preferentially on the (010) plane.<sup>9</sup> And  $\text{V}_2\text{O}_5$  was transformed to  $\text{V}_6\text{O}_{13}$  with losing a part of oxygens on the (010) plane.<sup>17</sup> We expected that the first reduction step  $\alpha$  might be related to the V-O species on the (010) plane.

We performed XPS analysis for the various vanadium oxides in order to find out how many kinds of oxygen species were there in these samples, and the results are shown in Figure 7. For the vanadium ion,  $\text{V}_{2p_{1/2}}$  appeared at 520.6 eV and  $\text{V}_{2p_{3/2}}$  appeared at 513.1 eV, and both the peaks did not show any changes with the samples. But for the oxygen ion, besides the main  $O_{1s}$  peak at 526.4 eV there was a shoulder peak at 529.5 eV. Labelling the shoulder peak as  $O_{1s}(\alpha)$  and the main peak as  $O_{1s}(\beta)$ , the peak intensity of  $O_{1s}(\alpha)$  changed with the samples and showed maximum intensity at V-4. We could calculate the area ratio of  $O_{1s}(\alpha)/O_{1s}(\beta)$  by using the method of curve fitting (a non-linear least square method assuming Gaussian peak shape), and the results are shown in Table 2. The change of  $O_{1s}(\alpha)/O_{1s}(\beta)$  with the samples showed a very similar trend to that of  $A(\alpha)/A(\beta)$ .

According to Andersson,<sup>14</sup> the unit cell of bulk  $\text{V}_2\text{O}_5$  crystal has one V-O and four V-O-V bonds. The oxygen( $O_{(1)}$ ) of V-O bond is 2-coordinated, and three oxygens( $O_{(2)}$ ) of V-O-V bonds which are sharing edges are 3-coordinated, and the last oxygen( $O_{(3)}$ ) of V-O-V bonds which is sharing corner is 2-coordinated. The average charge distributions were calcu-

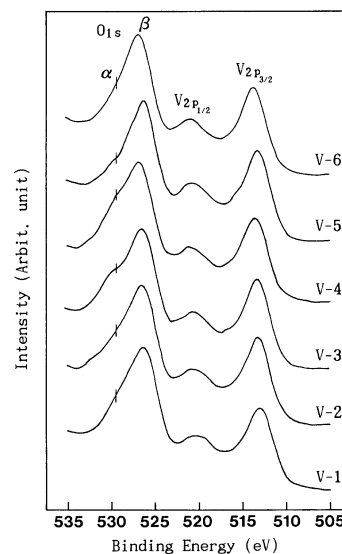
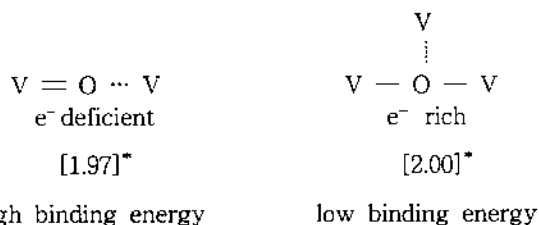


**Figure 7.** XPS spectra of various vanadium oxides showing the change of the shoulder peak at 529.5 eV.



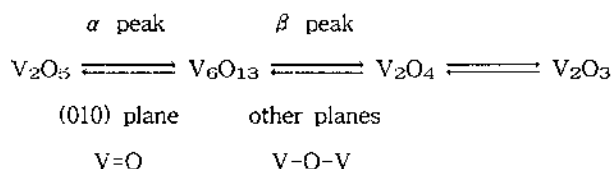
**Scheme 2.** Binding energies of the two different oxygen in  $\text{V}_2\text{O}_5$ . \*\* means the charge distribution around O in  $\text{V}_2\text{O}_5^{14}$ .

lated as  $\text{O}_{(1)}$ :1.97,  $\text{O}_{(2)}$ :2.00, and  $\text{O}_{(3)}$ :2.07, respectively. The oxygen of V-O showed the lowest value of charge distribution, which meant that  $\text{O}_{(1)}$  had lower electron density than the other two (Scheme 2). So  $\text{O}_{(1)}$  was expected to have higher binding energy in XPS spectrum than  $\text{O}_{(2)}$  or  $\text{O}_{(3)}$ . Therefore, we could conclude that the  $\text{O}_{1s}(\alpha)$  corresponded to the oxygen species of V-O and  $\text{O}_{1s}(\beta)$  was due to the convolution of  $\text{O}_{(2)}$  and  $\text{O}_{(3)}$ , namely, the oxygen species of V-O-V.

The changes of the morphological factor ( $I_{(101)}/I_{(010)}$ ), the ratio of  $\text{O}_{1s}$  peak area ( $\text{O}_{1s}(\alpha)/\text{O}_{1s}(\beta)$ ) in the XPS results, and the ratio of hydrogen consumption in TPR profiles with various vanadium oxides are shown in Figure 8 as a whole. We can see the distinct relationship between the structural property and their redox property of vanadium oxides. When the ratio of (010) plane increased,  $\text{O}_{1s}(\alpha)$  in XPS spectra and  $A(\alpha)$  in TPR profiles increased together. But when the ratio of (010) plane decreased, both the values decreased concurrently. We concluded that the oxygen species of V-O on (010) plane was removed on the first reduction step  $\alpha$  in TPR profiles but the second and the third reduction steps were due to the removal process of the other oxygen species of V-O-V. This is shown in the following Scheme 3.

**Catalytic oxidation of o-xylene.** The partial oxidation of o-xylene was selected as a model reaction in order to investigate the relation between the redox property of vanadium oxides and their catalytic property. Total conversions, yields, and selectivities of the catalytic reaction are shown in Table 3. The oxidation of o-xylene gave phthalic anhydride (PA) as a partial oxidation product, CO and  $\text{CO}_2$  ( $\text{C}_1$ ) as full oxidation products and some traces of o-tolualdehyde, phthalide, maleic anhydride, etc.

The total conversion of the reaction decreased from V-1 through V-4 and increased again after V-4, which was similar to the change of the surface areas in Table 1. The small conversion of V-4 was due to the low surface area. The yields of PA were constant with the samples, but those of  $\text{C}_1$  showed same trend to the change of the total conversion. As



**Scheme 3.** The relationship between the redox step and the structure of vanadium oxide.

**Table 3.** Conversions, Yields, and Selectivities of o-Xylene Oxidation over Various Vanadium Oxides

Catalysts	Total Conversion (molc%)	Yield (molc%)		Selectivity (molc%)	
		PA	$\text{C}_1$	PA	$\text{C}_1$
V-1	97.2	24.3	72.6	25.0	74.4
V-2	97.7	23.4	74.0	23.9	75.7
V-3	94.6	24.6	64.0	27.8	67.5
V-4	77.6	23.0	50.1	29.3	64.8
V-5	89.6	25.2	58.3	27.9	65.9
V-6	92.3	18.3	67.4	20.8	71.4

\*PA=phthalic anhydride,  $\text{C}_1$ =carbon monoxide and carbon dioxide. \*Reaction temperature=450 °C, space velocity=50 L-feed/hr : g-cat. and air/o-xylene mole ratio=100.

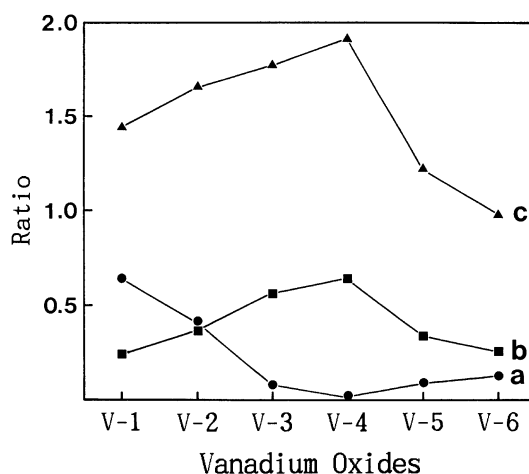


**Figure 8.** The change of (a) morphological factors ( $I_{(101)}/I_{(010)}$ ), (b) the ratio of  $\text{O}_{1s}$  peak area ( $\text{O}_{1s}(\alpha)/\text{O}_{1s}(\beta)$ ) in XPS result, and (c) the ratio of  $\text{H}_2$  consumption in TPR profiles with various vanadium oxides.

a result, V-4 showed the highest selectivity of PA because V-4 had a similar yield of PA but very low yield of  $\text{C}_1$ .

We thought that there were different surface oxygen spe-

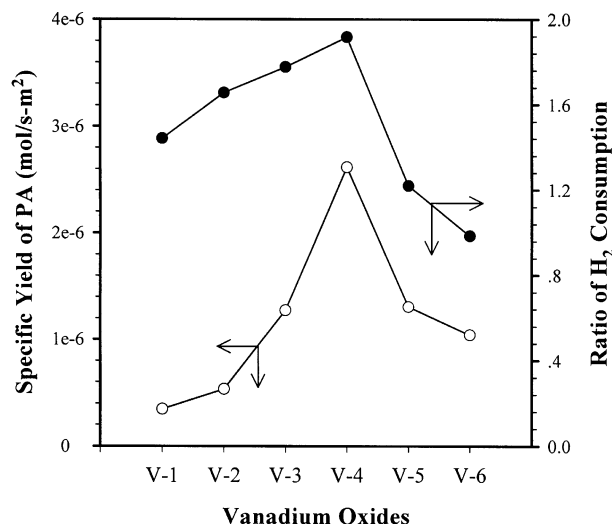


**Figure 9.** Specific yields of phthalic anhydride in the partial oxidation of o-xylene over various vanadium oxide catalysts (○) showing a similar trend to the change of  $\text{H}_2$  consumption ratio in TPR profiles (●).

cies for partial oxidation and full oxidation on vanadium oxides, and the ratio of the surface oxygen species for partial oxidation had the maximum value at V-4. The surface oxygen species could be differentiated by TPR, thus it would be a very interesting work to compare the yield of PA with the area ratio of the two reduction peaks in TPR profiles. It is shown in Figure 9. Here we used a specific yield, yield per unit surface area, because the catalytic activity depended on surface area. The change of specific yield showed a very similar trend to those of  $A(\alpha)/A(\beta)$ , which meant that the first reduction step related to the partial oxidation of o-xylene on vanadium oxide catalyst. Several authors reported that the oxygen species of V=O acted as active sites on the partial oxidation of o-xylene,<sup>7,21</sup> and our results showed a good agreement with it.

### Conclusions

The changes of the morphological factor ( $I_{(010)}/I_{(010)}$ ), the ratio of  $O_{1s}$  peak area ( $O_{1s}(\alpha)/O_{1s}(\beta)$ ) in the XPS results, and the ratio of hydrogen consumption in TPR profiles with various vanadium oxides showed the distinct relationship between the structural property and their redox property of vanadium oxides. For the partial oxidation of o-xylene, the redox property of vanadium oxides was correlated with their catalytic property. From the results presented in this experimental work the following useful informations could be provided.

1. In XRD patterns, vanadium oxides calcined near the melting point showed a large  $2\theta = 20.3^\circ$  peak which corresponded to (010) plane. Samples calcined below melting point were agglomerates of small grains of poorly defined shape, which grew to a needle-like crystal with the rise of calcination temperature. But other samples above melting point showed a multilayer structure of sheets.

2. All TPR profiles have two sharp peaks in the temperature range of 650-750 °C, and the intensity ratio of the two sharp peaks changed from sample to sample. The change of the ratio showed a similar trend to that of the morphological factor.

3. There were three redox steps in TPR/TPO profiles. The oxidation proceeded in the reverse order of reduction process, and both the reactions proceeded *via* quite a stable intermediates. The sharp reduction peaks seemed to be related to the shear transformation of vanadium oxides.

4. In XPS results the  $O_{1s}(\alpha)$  corresponded to the oxygen species of V=O and  $O_{1s}(\beta)$  was due to the oxygen species of V-O-V. The oxygen species of V=O on (010) plane was

removed on the first reduction step in TPR profiles but the second and the third reduction steps were due to the removal process of the other oxygen species of V-O-V.

5. The change in the specific yield of phthalic anhydride with various vanadium oxides showed a very similar trend to that of the peak area ratio in TPR profiles, which meant that the oxygen species of V=O on (010) plane related to the partial oxidation of o-xylene on vanadium oxide catalyst.

**Acknowledgment.** Financial support from the Korea Science and Engineering Foundation is greatly acknowledged.

### References

- Mars, P.; van Krevelen, D. W. *Chem. Eng. Sci. Spec. Suppl.* **1954**, *3*, 41.
- Bhattacharyya, S. K.; Mahanti, P. J. *Catal.* **1971**, *20*, 10.
- Gonzalez-Cruz, L.; Joly, J. P.; Germain, J. E. *J. Chem. Phys.* **1978**, *75*, 324.
- Bielanski, A.; Dyrek, K.; Serwicka, E. *J. Catal.* **1980**, *66*, 316.
- Tamura, K.; Yoshida, S.; Ishida, S.; Kakioka, H. *Bull. Soc. Chem. Jpn.* **1968**, *41*, 2840.
- Nakamura, M.; Kawai, K.; Fujiwara, Y. *J. Catal.* **1974**, *34*, 345.
- Cole, D. J.; Cullis, C. F.; Hucknall, D. J. *J. Chem. Soc. Faraday Trans. 1* **1976**, *72*, 2185.
- Akimoto, N.; Usami, M.; Echigoya, E. *Bull. Chem. Soc. Jpn.* **1978**, *51*, 2195.
- Bystrom, A.; Wilhelmi, K. A.; Brotzen, O. *Acta Chem. Scand.* **1950**, *4*, 1119.
- Kera, Y.; Hirota, K. *J. Phys. Chem.* **1969**, *73*, 3973.
- Gasior, M.; Machej, T. *J. Catal.* **1983**, *83*, 472.
- Robertson, S. D.; McNicol, B. D.; de Baas, J. H.; Kloet, S. C.; Jenkins, J. W. *J. Catal.* **1975**, *37*, 424.
- Lee, G.-D.; Lee, H.-I. *J. Korean Ind. & Eng. Chem.* **1991**, *2*, 155.
- Andersson, A. *J. Solid State Chem.* **1982**, *42*, 263.
- Zilkowski, J.; Janas, J. *J. Catal.* **1983**, *81*, 298.
- ASTM Powder Diffraction File*; JCPDS(ed.); Pennsylvania, U. S. A., 1979; pp 9-387.
- Haber, J. In *Catalysis*; Anderson, J. R., Boudart, M., Eds.; Springer-Verlag: Berlin, Germany, 1981; Vol. 2, p 13.
- Bielanski, A.; Haber, J. *Cat. Rev. Sci. Eng.* **1979**, *19*, 1.
- Andersson, A.; Andersson, S.; Lars, T. In *Solid State Chemistry in Catalysis*; Grasselli, R. K., Brazdil, J. F., Eds.; American Chemical Society: Washington, D. C., U. S. A., 1985; p 121.
- Dziembaj, R. *J. Solid State Chem.* **1978**, *26*, 159.
- Bond, G. C. *J. Catal.* **1989**, *116*, 531.